A R C H I V E S O F M E T A L L U R G Y A N D M A T E R I A L S
Volume 58 2013 Issue 4
DOI: 10.2478/amm-2013-0121

Y. HE*, W. ZHI*, C. RONG*

A THEORETICAL INVESTIGATION ON THE ELECTRON STRUCTURES OF Al-BASED INTERMETALLIC COMPOUNDS

TEORETYCZNE BADANIA STRUKTUR ELEKTRONOWYCH ZWIĄZKÓW MIĘDZYMETALICZNYCH NA BAZIE ALUMINIUM

Theoretical investigations were performed to study on alloying stability, and electronic structure of ($AlCu_3$, $AlCu_2Zr$ and $AlZr_3$). The results show that the lattice parameters obtained after full relaxation of crystalline cells are consistent with experimental data, and these intermetallics have a strong alloying ability and structural stability due to the negative formation energies and the cohesive energies. The further analysis find out that single-crystal elastic constants at zero-pressure satisfy the requirement of mechanical stability for cubic crystals. The calculations on Poisson's ratio show that $AlCu_3$ is much more anisotropic than the other two intermetallics. In addition, calculations on densities of states indicates that the valence bonds of these intermetallics are attributed to the valence electrons of Cu 3d states for $AlCu_3$, Cu 3d and Zr 4d states for $AlCu_2Zr$, and Al 3s, Zr 5s and 4d states for $AlZr_3$, respectively; in particular, the electronic structure of the $AlZr_3$ shows the strongest hybridization.

Keywords: intermetallic, first-principles, electron structure

Przeprowadzono teoretyczne badania stabilności stopów i struktury elektronowej $AlCu_3$, $AlCu_2Zr$ i $AlZr_3$). Obliczenia wskazują, że parametry sieci uzyskane po pełnej relaksacji komórek krystalicznych są zgodne z danymi eksperymentalnymi. Związki międzymetaliczne wykazują silną zdolność tworzenia stopów i stabilność strukturalną z powodu ujemnej energii tworzenia i energii spójności. Dalsze analizy wykazały, że stałe elastyczności pojedynczych kryształów przy zerowym ciśnieniu spełniają wymóg stabilności mechanicznej kryształów regularnych. Obliczenia współczynnika Poissona pokazują, że $AlCu_3$ posiada znacznie bardziej anizotropowe własności niż dwie pozostałe fazy mioędzymetaliczne. Ponadto, obliczenia gęstości stanów wskazują, że w tworzeniu faz międzymetalicznych biorą udział elektrony walencyjne odpowiednio: Cu na powłoce 3d dla $AlCu_3$, Cu na 3d i Zr na 4d dla $AlCu_2Zr$, oraz Al na 3s, Zr na 5s i 4d dla $AlZr_3$), w szczególności struktura elektronowa $AlZr_3$) wykazuje najsilniejszą hybrydyzację.

1. Introduction

Intermetallics involving aluminum and transition metals (TM) are known to have high resistance to oxidation and corrosion, elevated-temperature strength, relatively low density, and high melting points, which making them desirable candidates for high-temperature structural applications [1, 2]. In particular, Zirconium can effectively enhance the mechanical strength of the alloys when copper and zinc elements exist in aluminum and Al-based alloys [3]. Adding Zr in the Al-Mg alloys can effectively discard hydrogen, grain refinement, reducing pinholes, porosity and hot cracking tendency and improve its mechanical properties [4]. Many investigations have focused on the constituent binary systems, such as Al-Cu, Al-Zr, and Cu-Zr[5-10], however, there has been a lack of systematic theoretical and experimental investigations for binary and ternary system, especially for ternary alloy system.

In recent years, first-principles calculations based on the density-functional theory have become an important tool for the accurate study of the crystalline and electronic structures and mechanical properties of solids [11]. In the present study, we report a systematic investigation of the structural, elastic and electronic properties of Al-based alloys($AlCu_3$, $AlZr_3$ and $AlCu_2Zr$) by first-principles calculations, and the results are discussed in comparison with the available experimental data and other theoretical results.

2. Computational method

All calculations were performed using the Vienna ab initio Simulation Package (VASP) [12,13] based on the density-functional theory (DFT) [14]. The exchange and correlation energy was treated within the generalized gradient approximation of Perdew-Wang 91 version (GGA-PW91) [15].The interaction between the valence electrons and the ions was described by using potentials generated with Blöchl's projector augmented wave (PAW) method [16]. The PAW potential used for Al treats 3s, 3p states as valence states, and the other electron-ion interaction was described by 3d, 4s valence states for Cu, 5s, 4d ,5p valence states for Zr. A plane-wave energy cutoff was set at 450eV for $AlCu_3$ and

* SCHOOL OF MECHANICAL ENGINEERING, CHANGCHUN UNIVERSITY, CHANGCHUN 130022, P. R. CHINA

$AlCu_2Zr$, and at 350eV for $AlZr_3$. Brillouin Zone integrations were performed using the Monkhorst-Pack [17] k-point meshes, e.g., the k-point meshes for $AlCu_3$, $AlCu_2Zr$ and $AlZr_3$ were $15 \times 15 \times 15$, $9 \times 9 \times 9$ and $13 \times 13 \times 13$ for optimizing geometry and calculating elastic constants, and $25 \times 25 \times 25$, $19 \times 19 \times 19$ and $23 \times 23 \times 23$ for the calculations of density of states (DOS) at the equilibrium volume, respectively. Optimizations of the structural parameters (atomic positions and the lattice constants) for each system were performed using the conjugate gradient method, and the coordinates of internal atoms were allowed to relax until the total forces on each ion were less than 0.01 eV/Å. The total energy and density of states (DOS) calculations were performed with the linear tetrahedron method with Blöchl corrections [18]. In order to avoid wrap-around errors, all calculations were performed using the "accurate" setting within VASP.

3. Results and discussion

3.1. Equilibrium properties

$AlCu_3$ and $AlZr_3$ alloys have the simple cubic $Cu_3Au(L1_2$ type, space group Pm-3m) structure[19,20], $AlCu_2Zr$ alloy is a partially ordered Cu_2MnAl-type fcc structure with the Fm-3m space group[21]. Firstly, these crystal structures were optimized with relaxation of cell shape and atomic positions. The equilibrium volume V_0, bulk modulus B_0 and the pressure derivation of bulk modulus $B_0^{'}$ of $AlCu_3$,$AlCu_2Zr$ and $AlZr_3$ were determined by fitting the total energy calculated at different lattice constant values to a Birch-Murnaghan equation of state [22]. The results of first-principles calculations are listed in Table 1. From Table 1, one can see that the results of our calculations compare very favorably with experimental data. This shows that the used parameters are reasonable.

TABLE 1
Calculated and experimental lattice parameters a (Å), equilibrium volume V_0(Å^3), bulk modulus B_0(GPa) and the pressure derivation of bulk modulus $B_0^{'}$ for $AlCu_3$, $AlCu_2Zr$, $AlZr_3$

	$AlCu_3$		$AlCu_2Zr$		$AlZr_3$	
	Present.	Expt.	Present.	Expt.	Present.	Expt.
a	3.693	3.607[19]	6.256	6.216[21]	4.381	4.392[20]
V_0	50.358	–	244.805	240.210[21]	84.110	84.700[20]
B_0	131.010	–	128.600	–	100.800	101.4[7]
$B_0^{'}$	4.47	–	4.280	–	3.48	3.33[7]

It is known that the stability of crystal structure is correlated to its cohesive energy [23], which is often de?ned as the work which is needed when crystal is decomposed into the single atom. Hence, the lower the cohesive energy is, the more stable the crystal structure is [23]. In the present study, the cohesive energies (E_{coh}) of $AlCu_3$, $AlCu_2Zr$ and $AlZr_3$ crystal cells can be calculated by

$$E_{coh}^{ABC} = (E_{tot} - N_A E_{atom}^A - N_B E_{atom}^B - N_C E_{atom}^C)/(N_A + N_B + N_C) \quad (1)$$

where E_{tot} is the total energy of the compound at the equilibrium lattice constant, and E_{atom}^A, E_{atom}^B, E_{atom}^C are the energies of the isolated atoms A,B and C in the freedom states. N_A, N_B and N_C refer to the numbers of A, B and C atoms in each unit cell. The energies of isolated Al, Cu and Zr atoms are -0.276eV, -0.254eV and -2.054eV, respectively. Cohesive energies (E_{coh}) of per atom of all crystal or primitive cells are calculated from Eq. (1). It was found for Al-based intermetallic compounds that the cohesive energy (E_{coh}) of per atom for $AlCu_3$, $AlCu_2Zr$ and $AlZr_3$ are -3.637eV, -4.551eV, -5.964eV, respectively. These results are listed in Table 2. Based on the above results, it can be concluded that the cohesive energy of these Al-based intermetallic compounds will become lower with increasing Zr element in crystal, hence the stability of crystal increase. Therefore, the $AlZr_3$ intermetallic compound should have the highest structure stability, followed by $AlCu_2Zr$ and finally the $AlCu_3$.

TABLE 2
Total energyE_{tot}, cohesive energy E_{coh} and formation energy ΔH of $AlCu_3$, $AlCu_2Zr$ and $AlZr_3$

Compound	E_{tot}(eV/atom)	E_{coh} (eV/atom)	ΔH(eV /atom)
$AlCu_3$	-3.897	-3.637	-0.177
$AlCu_2$	Zr -5.261	-4.551	-0.359
$AlZr_3$	-7.574	-5.964	-0.307

In order to compare the alloying abilities of the present compounds, we calculate the formation energy ΔH, which can be given by

$$\Delta H_{ABC} = (E_{tot} - N_A E_{solid}^A - N_B E_{solid}^B - N_C E_{solid}^C)/(N_A + N_B + N_C) \quad (2)$$

where E_{solid}^A, E_{solid}^B and E_{solid}^C are the energies per atom of pure constituents A, B and C in the solid states, respectively. And the other variables are as defined for Eq. (1). If the formation energy is negative, the formation of a compound from its elements usually is an exothermic process. Furthermore, the lower the formation energy is, the stronger alloying ability is, and the more stable the crystal structure is [23]. The calculated energies of Al, Cu and Zr in their respective crystals are -3.696eV, -3.728eV, -8.457eV. The calculated results of these compounds are also listed in Table 2. As seen, all the ΔH is negative, which means that the structure of these compounds can exist and be stable. Further comparison and analysis showed that the alloying abilities of $AlCu_2Zr$ were much stronger than $AlCu_3$ and $AlZr_3$. It should be noticed that the alloying ability of $AlZr_3$ was higher than $AlCu_3$ alloy.

3.2. Elastic properties

The density-functional theory has become a powerful tool for investigating the elastic properties of materials (in the limit of zero temperature and in the absence of zero-point motion). For a given crystal it is possible to calculate the complete set of elastic constants by applying small strains to the equilibrium unit cell and determining the corresponding variations in the total energy. The necessary number of strains is imposed by the crystal symmetry[24]. For a material with cubic symmetry, there are only three independent elastic constants, C_{11} C_{12} and

C_{44}. And the strain tensor is given by

$$\delta = \begin{pmatrix} \delta_{11} & \delta_{12} & \delta_{13} \\ \delta_{21} & \delta_{22} & \delta_{23} \\ \delta_{31} & \delta_{32} & \delta_{33} \end{pmatrix} \tag{3}$$

In the present study, we applied three kinds of strains $\delta^{(N)}$ (N =1,2,3) so as to obtain the elastic constants, and they are listed in Table 3. The first strain is a volume-conserving tetragonal deformation along the z axis, the second refers to a uniform hydrostatic pressure, and the last one corresponds to a volume-conserving orthorhombic shear[24]. The elastic strain energy was given by

TABLE 3
The strains used to calculate the elastic constants of $AlCu_3$, $AlCu_2Zr$ and $AlZr_3$, with $\gamma = \pm 0.01n$ (n= 0 ~ 2)

Strain	Parameters(unlisted $\delta_{ij} = 0$)	$\Delta E/V_0$ to $0(\gamma^2)$
$\delta^{(1)}$	$\delta_{11} = \delta_{22} = \gamma, \delta_{33} = [(1+\gamma)^{-2} - 1]$	$3(C_{11} - C_{12})\gamma^2$
$\delta^{(2)}$	$\delta_{11} = \delta_{22} = \delta_{33} = \gamma$	$\frac{3}{2}(C_{11} + 2C_{12})\gamma^2$
$\delta^{(3)}$	$\delta_{12} = \delta_{21} = \gamma, \delta_{33} = [\gamma^2(1-\gamma^2)^{-1}]$	$2C_{44}\gamma^2$

$$U = \frac{\Delta E}{V_0} = \frac{1}{2}\sum_{i=1}^{6}\sum_{j=1}^{6} C_{ij}e_i e_j \tag{4}$$

where $\Delta E = E_{total}(V_0, \delta) - E_{total}(V_0, 0)$ is the total energy variation between the deformed cell and the initial cell, V_0 is the equilibrium volume of the cell, C_{ij} is the elastic constants and δ is the deformation added to the equilibrium cell. The elastic strain energy is also listed in Table 3. For each kind of lattice deformation, the total energy has been calculated for different strains $\gamma = \pm 0.01n$(n= 0 ~ 2). By means of polynomial fit, we extracted three values of the second order coefficients, corresponding to $3(C_{11}-C_{12})$, $3(C_{11}+2C_{12})/2$ and $2C_{44}$, respectively, the elastic constants C_{11} C_{12} and C_{44} were obtained[25], and the results are showed in Table 4. From Table 4, we can see that our calculation results agree well with the experimental data or other first-principle calculations. These elastic constants satisfy the requirement of mechanical stability for cubic crystals [24]: $(C_{11} - C_{12}) > 0$, $C_{11} > 0$, $C_{44} > 0$, $(C_{11} + 2C_{12}) > 0$. This shows that $AlCu_3$, $AlCu_2Zr$ and $AlZr_3$ have a stable structure. The average bulk modulus is identical to the single-crystal bulk modulus, i.e., $B = (C_{11} + 2C_{12})/3$. Interestingly, we noted that the bulk modulus calculated from the values of the elastic constants is in good agreement with the one obtained through the fitting to a Birch-Murnaghan equation of state (B_0), giving a consistent estimation of the compressibility for these compounds [26].

In order to further validate our results, the elastic modulus, such as shear modulus G(GPa), Young's modulus E(GPa), Poisson's ratio ν and anisotropy constant A for a polycrystalline material were also calculated with the single-crystal elastic constants C_{ij}, all of these elastic modulus are shown in Table 4. In the present study, we adopted Hershey's averaging method [27], which has been known to give the most accurate relation between single-crystal and polycrystalline values for a cubic lattice [28]. According to this method, G is obtained by solving the following equation:

$$G^3 + \frac{5C_{11} + 4C_{12}}{8}G^2 - \frac{C_{44}(7C_{11} - 4C_{12})}{8} G - \frac{C_{44}(C_{11} - C_{12})(C_{11} + 2C_{12})}{8} = 0 \tag{5}$$

The calculated shear modulus G for the $AlZr_3$ are the largest, while the quantities for $AlCu_2Zr$ are less than for $AlCu_3$.

Pugh [29] found that the ratio of the bulk modulus to shear modulus (B/G) of polycrystalline phases can predict the brittle and ductile behavior of materials. A high and low value of B/G are associated with ductility and brittleness, respectively. The critical value which separates ductility from brittleness is about 1.75. From B/G calculated in Table 4 we can see that all the B/G ratios are larger than 1.75. Therefore, $AlCu_3$, $AlCu_2Zr$ and $AlZr_3$ have a good ductility. On the contrary, the biggest B/G ratio for $AlCu_2Zr$ indicates that $AlCu_2Zr$ is of very good ductility in these three Al-based alloys. $AlCu_3$ has an intermediate ductility, while $AlZr_3$ has a worst ductility.

Besides B/G, Young's modulus E and Poisson's ratio ν, which are important for technological and engineering applications. Young's modulus is used to provide a measure of the stiffness of the solid, i.e., the larger the value of E, the stiffer the material [24]. According to Hershey's averaging method, Young's modulus is defined as: $E = 9GB/(3B + G)$. Based on the calculated results, we find that $AlZr_3$ has a Young's modulus that is 18.806GPa and 24.663GPa larger than $AlCu_3$ and $AlCu_2Zr$, respectively. This indicates that $AlZr_3$ phase has the highest stiffness, followed by $AlCu_3$ and finally the $AlCu_2Zr$.

TABLE 4
Calculate elastic constants (GPa) and elastic modulus (bulk modulus B(GPa), shear modulus G(GPa), Young's modulus E(GPa), Poisson's ratio ν and anisotropy constant A) of $AlCu_3$,$AlCu_2Zr$ and $AlZr_3$

Compound	C_{11}	C_{12}	C_{44}	B	G	B/G	E	ν	A	reference
$AlCu_3$	150.707	120.565	81.880	130.612	43.593	2.996	117.686	0.350	1.887	this study
	176.000	117.400	92.400	136.900	49.600		132.800	0.340		[5]
$AlCu_2Zr$	157.504	115.305	62.685	129.371	41.237	3.137	111.829	0.356	1.528	this study
$AlZr_3$	148.653	79.387	70.834	102.476	53.400	1.919	136.492	0.278	1.487	this study
	163.800	79.300	86.500	107.670						[6]

In addition, Poisson's ratio ν has also been used to measure the shear stability of the lattice, which usually ranges from -1 to 0.5. The greater the value of Poisson's ratio ν, the better the plasticity of the materials. So we can see that $AlCu_3$, $AlCu_2Zr$ and $AlZr_3$ have a better plasticity.

The elastic anisotropy of crystals has an important application in engineering materials since it is highly correlated with the possibility of inducing microcracks [24,30]. For cubic symmetric structures [31], the elastic anisotropy is defined as $A = (2C_{44} + C_{12})/C_{11}$. For the completely isotropic material, the value of A will be 1, while values smaller or bigger than 1 measuring the degree of elastic anisotropy [24]. Interestingly, we note that the values of A (Table 4) do not deviate far from unity, suggesting that the present cubic structure alloys also do not deviate far from being isotropic. The calculated results also indicate that $AlCu_3$ is much more anisotropic than the other two alloys.

3.3. Density of the states

For further understanding of the electronic characteristic and structural stability, total density of states (DOS) of $AlCu_3$, $AlCu_2Zr$ and $AlZr_3$ were calculated, as shown in Fig. 1, as well as the partial density of states (PDOS) of Al, Cu and Zr atoms in these Al-based intermetallics compounds. Fig. 1 is evident the metallic character of these considered $AlCu_3$, $AlCu_2Zr$ and $AlZr_3$ structure because of the finite DOS at the Fermi level. With regard to the total density of states curve of $AlCu_3$, one can see from Fig. 1a that the whole valence band of $AlCu_3$ is located between -7eV and 9eV, which is dominated by Cu 3d states and a small contribution from 3s and 3p states of Al. The valence band of $AlZr_3$ (see Fig. 1c) can be divided into three areas. The first area dominated by the valence electron numbers of Al 3s and Zr 4d states are mostly located between -7eV and -5eV, the second by the Zr 5s and 4d states located between -4eV and -3eV, and the third by Zr 4d states located between -2.8eV and 3.0eV. Both below and above the Fermi level, the hybridization between Al-p states and Zr-d states is strong. Due to the strong hybridization (or covalent interaction) the entire DOS can be devided into bonding and antibonding regions, and that a pseudogap resides in between. The characteristic pseudogap around the Fermi level indicates the presence of the directional covalent bonding. The Fermi level located at a valley in the bonding region implies the system has a pronounced stability. It is also generally considered that the formation of covalent bonding would enhance the strength of material in comparison with the pure metallic bonding [32]. According to the covalent approach, the guiding principle is the maximize bonding. Therefore, for a series of compounds having the same structure, the greater the occupancy in the bonding region the higher the stability [33]. It is indeed seen that the structural stability increases from $AlCu_3$ to $AlZr_3$. For $AlCu_2Zr$ (see Fig. 1b), it is found that the main bonding peaks between -6eV and -2eV are predominantly derived from the Cu 3d orbits, while the main bonding peaks between the Fermi level and 3eV predominantly derived from the Zr 4d orbits. It should be noted that the phase stability of intermetallics depends on the location of the Fermi level and the value of the DOS at the Fermi level, i.e. $N(E_F)$ [34,35]. A lower $N(E_F)$ corresponds to a more stable structure. The value of the total DOS at the Fermi level is 3.64 states/eV for $AlZr_3$. And the value of the total DOS at the Fermi level is 5.74 states/eV for $AlCu_2Zr$. Therefore, $AlZr_3$ has a more stable structure in these three Al-based intermetallics. This accorded with the the calculation of cohesive energy.

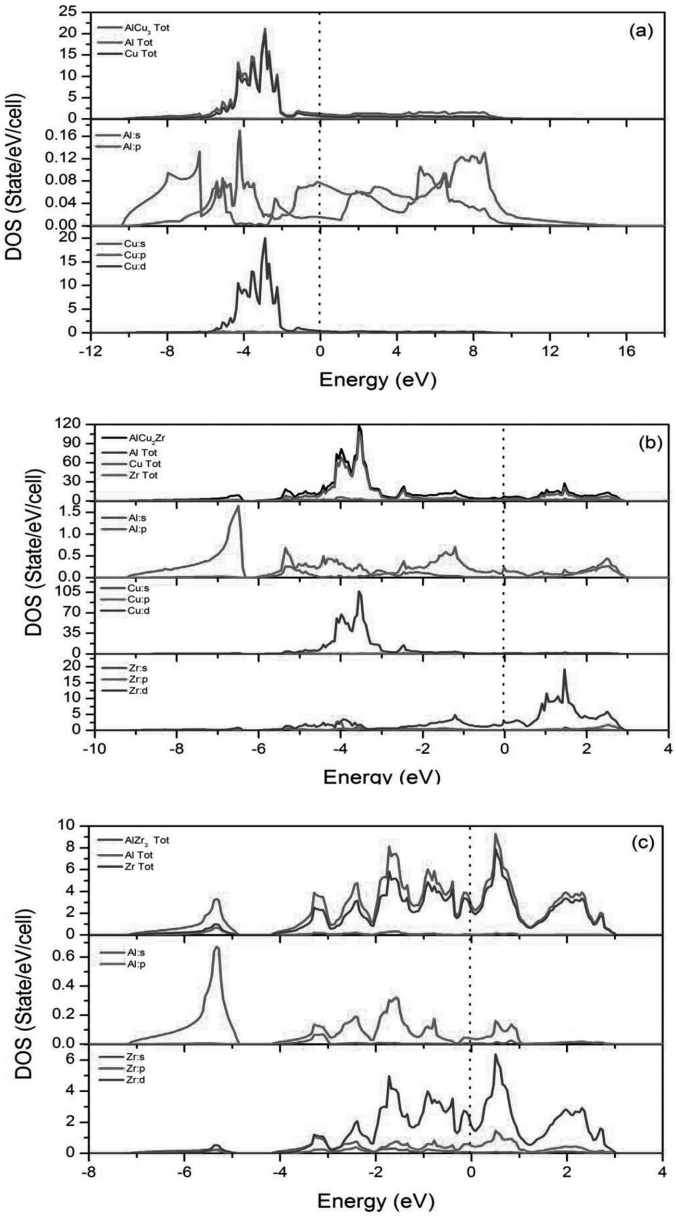

Fig. 1. The total and partial density of states (DOS) of $AlCu_3$ crystal cell (a), $AlCu_2Zr$ crystal cell (b), $AlZr_3$ crystal cell (c). The vertical dot line indicates the Fermi level

4. Conclusions

In summary, using the first-principles method we have calculated alloying stability, electronic structure, and mechanical properties of $AlCu_3$, $AlCu_2Zr$ and $AlZr_3$. These intermetallics have a strong alloying ability and structural stability due to the negative formation energies and the cohesive energies. In particular, $AlCu_3$ is much more anisotropic than the other two intermetallics. The valence bonds of these intermetallics are attributed to the valence electrons of Cu 3d

states for $AlCu_3$, Cu 3d and Zr 4d states for $AlCu_2Zr$, and Al 3s, Zr 5s and 4d states for $AlZr_3$, respectively, and the electronic structure of the $AlZr_3$ shows the strongest hybridization, leading to the worst ductility.

REFERENCES

[1] G. Sauthoff, In: Westbrook JH, Fleischer RL, editors. Intermetallic compounds, New York (NY): Wiley **1**, 991 (1994).
[2] R.W. Cahn, Intermetallics **6**, 563-569 (1998).
[3] P.K. Rajagopalan, I.G. Sharma, T.S. Krishnan, J Alloys Compd **285**, 212-217 (1999).
[4] P. Wonwook, Mater Design **17**, 85-90 (1996).
[5] W. Zhou, L.J. Liu, B.L. Li, J Electron Mater **38**, 356-359 (2009).
[6] C. Emmanuel, J.M. Sanchez, Phys Rev B **65**, 094105-09412 (2002).
[7] G. Ghosh, Acta Mater **53**, 3225-3234 (2005).
[8] G. Ghosh, Acta Mater **55**, 3347-3354 (2007).
[9] W.J. Ma, Y.R. Wang, B.C. Wei, Trans Nonferrous Met Soc China **17**, 929-933 (2007).
[10] S. Pauly, J. Das, N. Mattern, Intermetallics **17**, 453-458 (2009).
[11] H. Baltache, R. Khenata, M. Sahnoun, Physica B **344**, 334-337 (2004).
[12] G. Kresse, J. Hafner, Phys Rev B **49**, 14251-14258 (1994).
[13] G. Kresse, J. Furthmüller, Phys Rev B **54**, 11169-11175 (1996).
[14] W. Kohn, L.J. Sham, Phys Rev **140**, A1133-1138 (1965).
[15] J.P. Perdw, Y. Wang, Phys Rev B **45**, 13244-13247 (1992).
[16] P.E. Blöchl, Phys Rev B **50**, 17953-17959 (1994).
[17] H.J. Monkhorst, J.D. Pack, Phys Rev B **13**, 5188-5195 (1996).
[18] P.E. Blöchl, O. Jepsen, O.K. Andersen, Phys Rev B **49**, 16223-16228 (1994).
[19] M. Draissia, M.Y. Debili, N. Boukhris, Copper **10**, 65-69 (2007).
[20] W.J. Meng, J.J. Faber, P.R. Okamoto, J Appl Phys **67**, 1312-1318 (1990).
[21] M. Reckendorf, P.C. Schmidt, A.Z. Weiss, Phys Chem **163**, 103-108 (1989).
[22] F. Birch, J Geophys Res **83**, 1257-1263 (1978).
[23] V.I. Zubov, N.P. Tretiakov, Phys Lett A **194**, 223228 (1994).
[24] M. Mattesini, R. Ahuja, B. Johansson, Phys Rev B **68**, 184108-184113 (2003).
[25] W.Y. Yu, N. Wang, X.B. Xiao, Solid State Sciences **11**, 1400-1406 (2009).
[26] B.Y. Tang, N. Wang, W.Y. Yu, Acta Mater **56**, 3353-3358 (2008).
[27] H.M. Ledbetter, J Appl Phys **44**, 1451-1457 (1973).
[28] A. Taga, L. Vitos, B. Johansson, Phys Rev B **71**, 014201-014207 (2005).
[29] S.F. Pugh, Philos Mag **45**, 823-829 (1954).
[30] V. Tvergaard, J.W. Hutchinson, J Am Ceram Soc **71**, 157-164 (1988).
[31] B.B. Karki, L. Stixrude, S.J. Clark, J. Am Miner **82**, 51-58 (1997).
[32] P. Chen, D.L. Li, J.X. Yi, Solid State Sciences **11**, 2156-2162 (2009).
[33] J.H. Xu, W. Lin, A.J. Freeman, Phys Rev B **48**, 4276-4283 (1993).
[34] J.H. Xu, T. Oguchi, A.J. Freeman, Phys Rev B **36**, 4186-4293 (1987).
[35] T. Hong, T.J. Yang, A.J. Freeman, Phys Rev B **41**, 12462-12470 (1990).

Received: 10 April 2012.